Astronomical Notes

Astronomische Nachrichten

Founded by H. C. Schumacher in 1821

WILEY-VCH

REPRINT

Astron. Nachr. / AN **334**, No. 8, 828 – 831 (2013) / **DOI** 10.1002/asna.201311931

Expected characteristics of data from the LYRA mission

A.I. Zakharov*, **A.V. Mironov, M.E. Prokhorov, F.N. Nikolaev, M.S. Tuchin,** and **A.V. Biryukov**

Sternberg Astronomical Institute, Lomonosov Moscow State University, Universitetsky Prospect 13, 119991 Moscow, Russia

Received 2013 Apr 3, accepted 2013 Jun 7
Published online 2013 Oct 1

Key words instrumentation: photometers – stars: fundamental parameters – surveys – techniques: photometric – telescopes

The purpose of the LYRA mission is a multi-color all-sky survey of objects from $3^{\rm m}$ to $16^{\rm m}$ from the International Space Station, to result in a high-precision photometric catalog (Zakharov et al. 2013b). The expected error of the catalog will be $0.001-0.003^{\rm m}$ for stars brighter than $12^{\rm m}$ and $0.01^{\rm m}$ for the stars down to $16^{\rm m}$. The estimated duration of the survey is about 5 years. This paper describes the characteristics of data to be received in the course of the LYRA experiment for future users.

1 Equipment and principles of the survey

The LYRA experiment will use a telescope with the mirror diameter of 0.5 m and the focal length of 3 m, built according to a quasi-Ritchey-Chretien scheme. In the focal plane of the telescope, a mosaic of 22 CCDs with 11 different filters is located. The telescope will make observations in a scanning mode, and the CCDs will detect images in the TDI (Time Delay and Integration) mode. To do this, the telescope is fixed with respect of the body of the International Space Station (ISS), and CCD mosaic columns are oriented along the direction of star-image motion.

Scanning is performed by the orbital motion of the ISS, during which the ISS has an orientation with one axis of the station always facing the Earth and another axis directed along the orbit. As a result, the station makes one turn around the third axis in the time of one orbital revolution. The rotation of the station leads to changing orientation of the telescope, with a displacement of star images in the focal plane. The main orientation of the telescope's sighting axis lies in the plane of the orbit of the ISS. During one revolution, the sky is scanned along a great circle band with a width of 1° (actual observations are made only on the part of the loop where illumination from the Sun is small). The ISS orbital inclination is 51.6°. Because of the orbit precession, the nodes of the orbit move by 0.3° in one orbital revolution. This shift is smaller than the width of the scanning strip. The combination of orbital and precession motion permits to observe all objects with $|\delta| < 51.6^\circ$ (see Fig. 1, left part).

To observe the polar regions, the telescope axis should be inclined by 38.4° to the north or south, and the scan will go along a small circle of the celestial sphere that passes through the celestial pole (see Fig. 1, right part). The combination of these three modes makes observations cover the entire celestial sphere.

If the observations are performed during 50 % of all time, the annual average number of observations for a point of the celestial sphere is 22, and in 5 years, 110.

2 Structure and functioning of the focal plane

In the focal plane of the LYRA telescope, 22 CCDs, 2250×300 pixels in size, are located. The pixel size is 12 μm ($0.8''$). Images of stars move along the short side of the CCD. In the mosaic, pairs of CCDs with similar filter coating are collected by two in one case and joined by the short side (see Fig. 2). During scanning in small circles, these CCDs are given different TDI frequency to reduce image blurring. The optical system is made so that the PSF size is of the order of 1.5–2 pixels across the entire field of view.

Panchromatic antireflection coating covers the first CCD (in the direction of star-image motion). This CCD is used for detection of objects observed in the field of view, the survey being performed without an input catalog of stars. On the other CCDs, interference coatings are deposited implementing the LYRA photometric system that covers the range between 195 and 930 nm. The parameters of the photometric system's spectral bands are presented in Table 1. Coating being located directly on the CCDs avoids glare from bright stars and simultaneously reduces reflection from the surface of a silicon CCD. The method of coating silicon was developed in the Lebedev Physics Institute and tested on the Coronas satellites.

For stars detected on the first CCD, positions and times of appearance on all other CCDs are predicted. Around the

* Corresponding author: zakh@sai.msu.ru

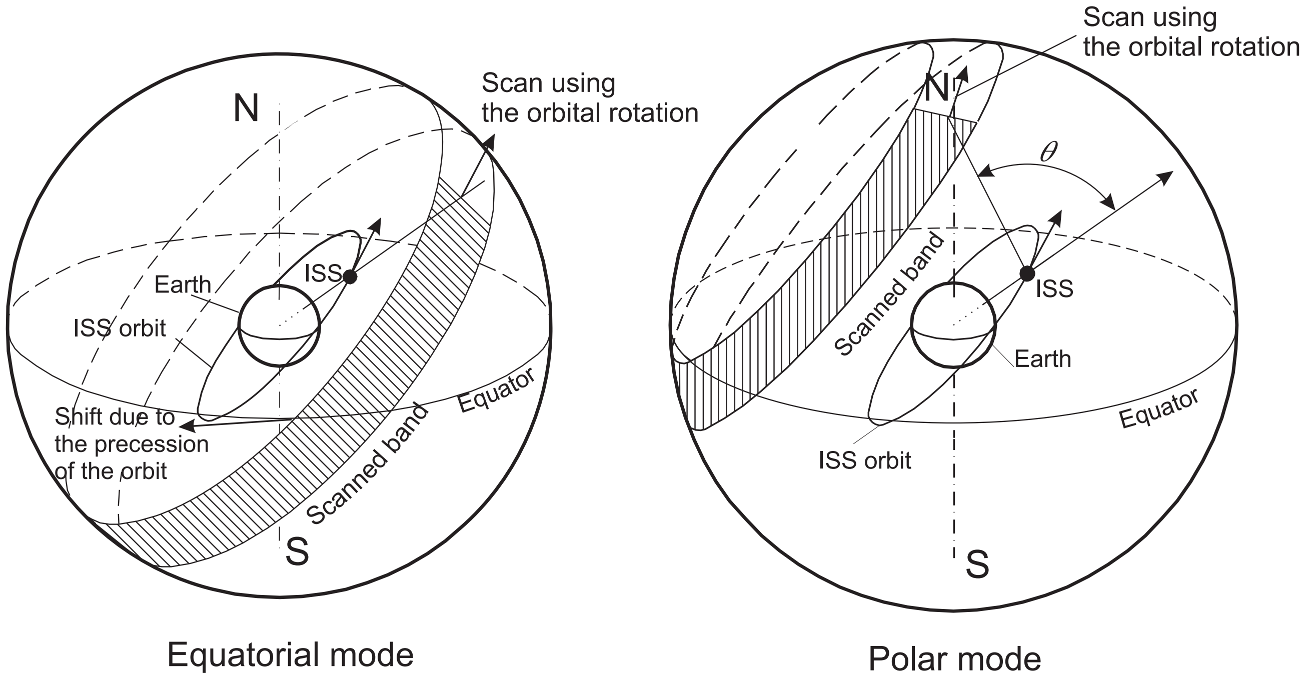

Fig. 1 Scanning the sky. *Left*: scanning in the case of the principal orientation of the instrument, i.e. with the telescope axis in the orbital plane. *Right*: the telescope axis is moved by 38.4° to the north, and the scanned strip covers the north celestial pole.

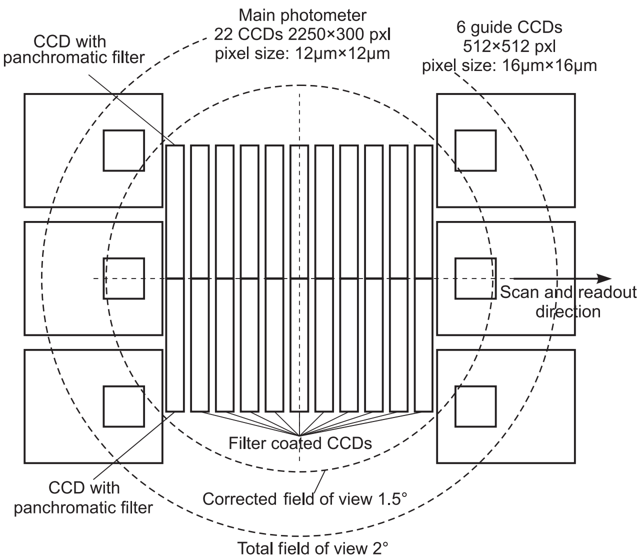

Fig. 2 Design of the focal plane in the LYRA experiment.

expected position, a fragment of the image (presumably $7{\times}7$ pixels) is selected and saved for later processing. The rest of sky image between the fragments is averaged along $1{\times}100$–150-pixel rows for estimation of sky background.

3 The LYRA photometric system and limiting magnitudes

The central wavelengths of the photometric bands in the current version of the LYRA photometric system are the following: 195, 218, 270, 350, 374, 440, 550, 700, 825, and 930 nm (Zakharov et al. 2013a). The first three bands lie in the ultraviolet; 218 nm is the wavelength of the center of an interstellar-extinction band, with two other bands' spectral transmission centered before and after it. 350, 440, 550, and 700 nm are the wavelengths of the midpoints of the standard photometric $WBVR$ bands of Johnson's system (Johnson & Morgan 1953), the system used in the high-precision catalog of $WBVR$ magnitudes of bright stars in the northern sky (Kornilov et al. 1991). The filter centered at 374 nm falls on the Balmer jump. The band centered at 825 nm corresponds to a TiO absorption band and permits to determine metallicities of stars. The 930 nm filter is located around a water-vapor absorption band in the atmosphere. The panchromatic band transmits radiation in the range from 400 to 900 nm.

The photometric bands are shown in Fig. 3, and Table 1 presents the limiting magnitudes expected in the LYRA survey.

Table 1 Limiting magnitudes of the LYRA survey.

λ_0	$\Delta\lambda$	Faintest Objects: One Observation		Five Years	CCD
		$0.01^{\rm m}(1\%)$	$0.1^{\rm m}(10\%)$	$0.01^{\rm m}(1\%)$	Over-
(nm)	(nm)				flow
195	20	8.96	13.58	13.66	6.02
218	20	8.93	13.56	13.64	6.00
270	25	9.15	13.77	13.85	6.22
350	50	10.46	15.10	15.18	7.54
440	100	12.48	16.91	16.98	8.80
550	80	11.67	16.10	16.17	7.99
700	80	10.72	15.02	15.09	6.61
825	80	9.73	14.03	14.10	5.62
930	80	8.67	12.87	12.94	4.25
Panchrom.	∼500	14.16	18.36	—	9.74

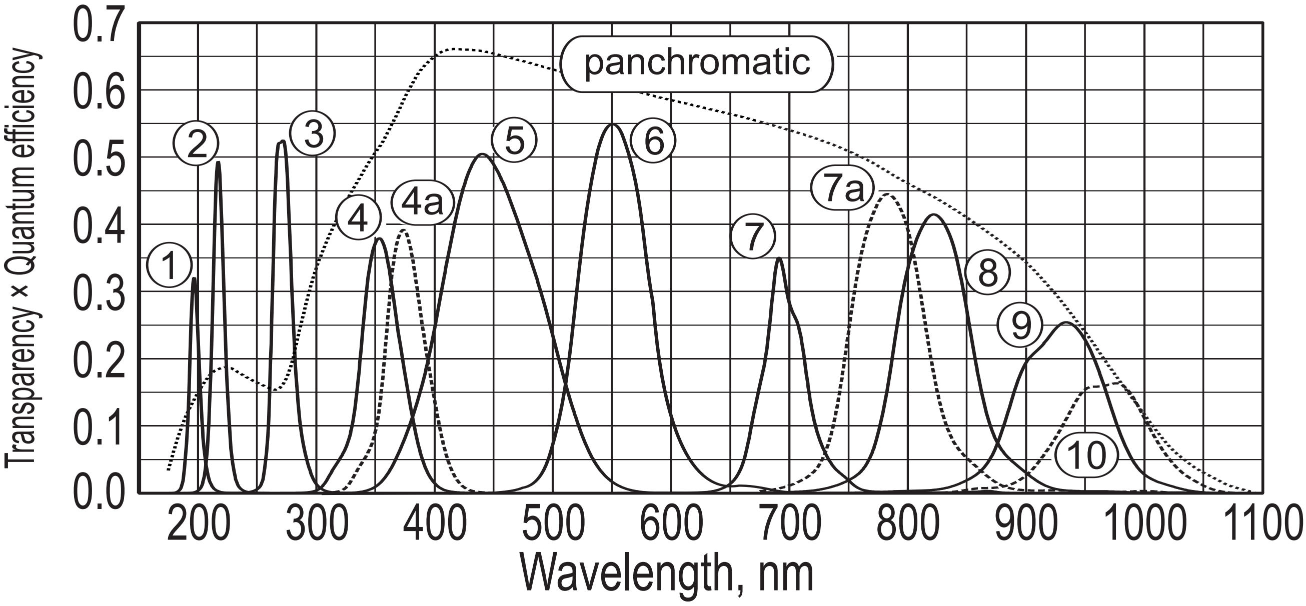

Fig. 3 The passbands of the LYRA photometric system, with the central wavelengths 195 nm (1), 218 nm (2), 270 nm (3), 350 nm (4), 374 nm (4a), 440 nm(5), 555 nm (6), 700 nm (7), 785 nm (7a), 825 nm (8), 930 nm (9), 1000 nm (10), and the broadband panchromatic filter. The passbands take into account the transmission of the interference filter covering the silicon surface and the CCD quantum efficiency.

4 Registration of the brightest stars

It appears from Table 1 that the brightest stars (brighter than 4–$9^{\rm m}$ in different bands) overflow the CCD pixels during the exposure. For registration of such stars, a special mode is used. Images are defocused to 10–15 pixels. The total capacity of pixels on which the image of the star is placed increases by a factor of about 100, which leads to a shift in the dynamic range of detected objects by $5^{\rm m}$ towards bright stars. We intend to use this mode at the beginning and end of observing sessions, when the solar illumination increases.

5 Observation time scales

There are three time scales present in observations of stars. The first time scale is associated with the passage of a star over the focal plane. When scanning in the plane of the ISS orbit, the crossing time of all the 11 CCDs is 15 s. One CCD is crossed in 1.05 s. The time between observations on the neighboring CCDs is 1.4 s. These times increase by 25 % in the polar scan mode.

The second time scale is associated with the orbital motion of the ISS. Any star will be observed on at least five consecutive orbits. The time interval between observations is the same as the orbital period of the ISS: 1.5 hours.

The third time scale is associated with the re-hit of the object field of view. This time is approximately one month. Since the orientation of the telescope is changed also approximately once per month, this is a quasi-periodic time scale.

6 Irremovable blur of images

In the polar scanning mode, images on opposite ends of a CCD are moving at different speeds, and trajectories of star images are arcs. Because of these effects, an irremovable image blur appears. When selecting the optimal TDI frequency corresponding to the central column of the CCD, the longitudinal blur in the outer columns of the CCD is 1 pixel. The transverse blur is 3 pixels for the first and last CCDs; 1.5 pixels for the second and penultimate CCDs; and less than 1 pixel for the others.

When scanning in the orbital plane, the irremovable blur is negligible.

7 Coverage of the sky, number of observations, number of stars in the survey

Simulations show that it is possible to observe the entire celestial sphere in one year. In addition, each object is observed, on average, 22 times; near the poles, this number will increase to 1000. Within 5 years of the experiment, an average of 110 measurements will be obtained for each object.

The expected number of stars that will be recorded in the survey ranges from 100 to 400 millions. This estimate is derived from the 2MASS (Skrutskie et al. 2006) and USNO-B1.0 (Monet et al. 2003) data. The main uncertainty is from poor knowledge of the interstellar absorption in the galactic plane.

Table 2 The characteristics of the LYRA mission that will not change.

Characteristic	Reason
Scanning mode of observations	(1) Reliability of the design: most time the telescope is fixed with respect of the station. (2) Averaging of CCD characteristics along the columns. (3) Stable operation modes of the CCDs and electronics.
Diameter of the telescope (0.5 m)	Limitations on the delivery by ISS construction (delivery through the habitable zone of the ISS).
Field of view width (scan width)	Making it narrower: deteriorating coverage of the celestial sphere. Making it wider: reducing the quality of the optical system.
CCD pixel size (12 μm)	Capacity of the pixel. Technological limitations.
Number of spectral bands (11)	More bands: problems with focal plane construction. Fewer bands: no win.

8 Positions of stars in the LYRA survey

Random errors of the relative coordinates of stars simultaneously detected in the focal plane (i.e. with distances from each other less than 1°) are about 100 μas for bright stars and about 1 mas for other stars. The contribution of systematic errors and the possibility of building the global coordinate system from these data need a further study.

9 What can and cannot be changed in the LYRA experiment?

The characteristics that, most likely, will not change or will change only slightly are presented in Table 2. The characteristics that can be changed are

- the algorithm of celestial sphere coverage,
- central wavelengths, widths, and profiles of photometric bands,
- the threshold of star detection,
- processing of the background measurements.

10 GAIA and LYRA or GAIA plus LYRA

The experiments GAIA (Perryman 2005) and LYRA will be performed almost simultaneously (the planned beginning of GAIA is 2013 and that of LYRA 2015) and measure the same stars. Very precise Gaia astrometry and good Lyra photometry will be obtained down to 12^{m}; then, both missions will provide good astrometry and photometry down to 17^{m}. Combining data from these surveys will permit to create a universal catalog of a higher class than in each of them separately.

References

Johnson, H.L., & Morgan, W.W. 1953, ApJ, 117, 313
Kornilov, V.G., Volkov, I.M., Zakharov, A.I., et al. 1991, Trudy Gosud. Astron. Sternberga (Proc. of the Sternberg Astron. Inst.), 63, 1
Monet, D.G., Levine, S.E., Casian, B., et al. 2003, AJ, 125, 984
Perryman, M.A.C. 2005, Overview of the Gaia Mission, in The Three-Dimensional Universe with Gaia, ed. C. Turon, K. S. O'Flaherty, & M. A. C. Perryman, ESA SP-576 (ESA-ESTEC, Noordwijk), 15
Skrutskie, M.F., Cutri, R.M., Stiening, R., et al. 2006, AJ, 131, 1163
Zakharov, A.I., Mironov, A.V., Nikolaev, F.N., Prokhorov, M.E., & Tuchin, M.S. 2013a, Astron. Nachr., 334, 823
Zakharov, A.I., Mironov, A.V., Prokhorov, M.E., et al. 2013b, Astronomy Reports, 57, 195